



Supplement of

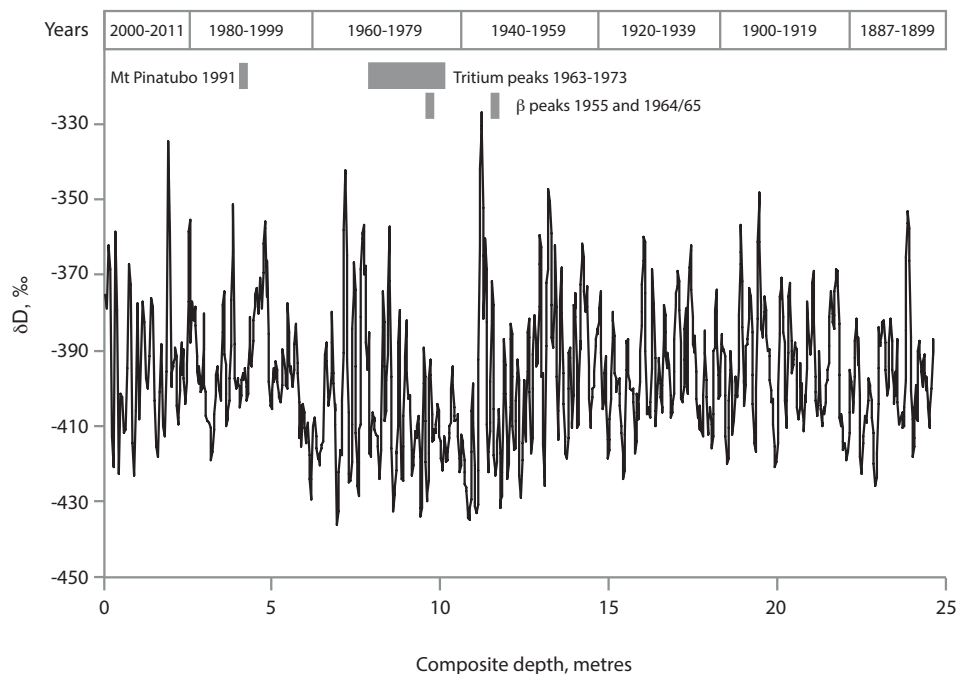
Tropical and mid-latitude forcing of continental Antarctic temperatures

C. S. M. Turney et al.

Correspondence to: C. S. M. Turney (c.turney@unsw.edu.au)

The copyright of individual parts of the supplement might differ from the CC-BY 3.0 licence.

1 *Text S1: 2012 South Geographic Pole core*



2

3 **Figure S1:** South Geographic Pole δD values on common depth scale with
4 chronology, compiled from present study and previous work (Jouzel et al., 1983).
5 Independent checks on chronology are provided by the tropical 1991 eruption of
6 Mount Pinatubo and/or the Cerro Hudson (identified by a prominent non-sea salt
7 sulfate peak) and known tritium and β peaks.

8
9

10

11

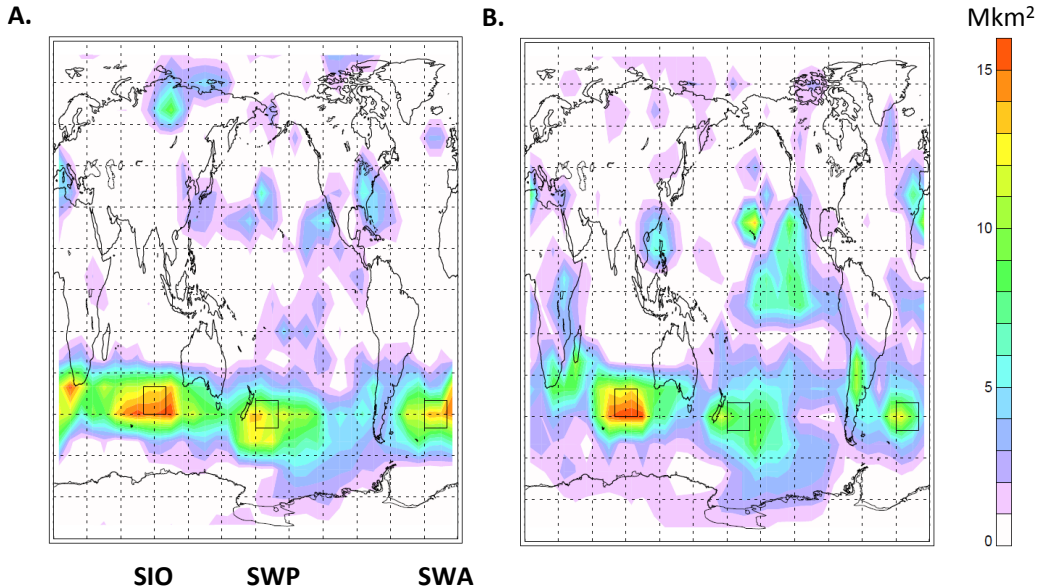
12

13

14

15 *Text S2: Spatial Controls on Antarctic Warming*

16 The same relationship observed between the surface pressure anomalies and
17 temperature extends up to 700 hPa (Figure S2).



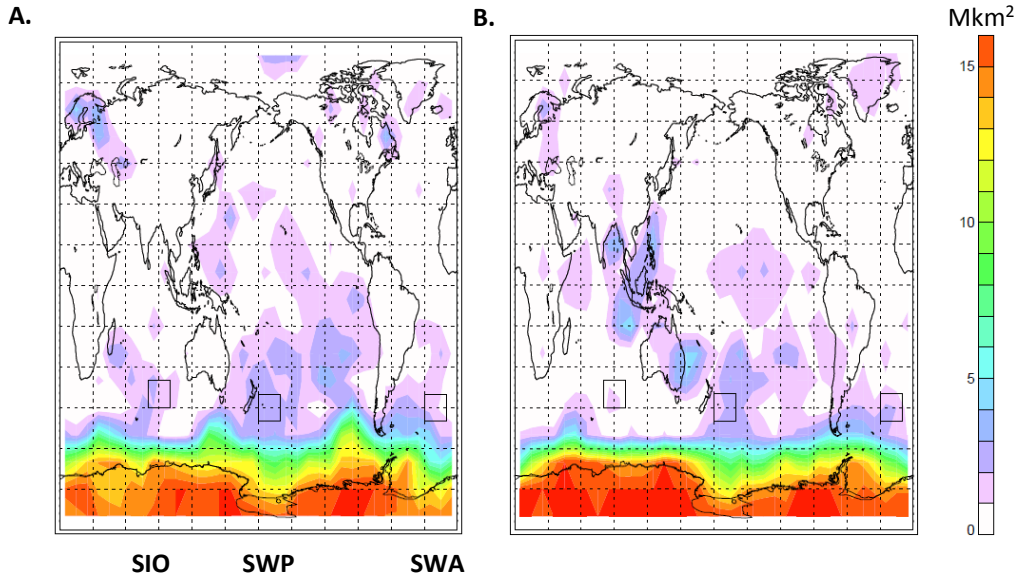
18

19 **Figure S2:** Panel A. The cumulative area of significant positive 700 hPa temperature
20 anomalies poleward of 65°S (in million km²) produced by compositing months having
21 negative 700 hPa geopotential height anomalies (thresholded at the 10th percentile) in
22 each 10° x 10° (longitude x latitude) box, obtained from deseasonalised monthly
23 ERA-Interim reanalysis data for 1979-2012 (Dee et al., 2011). The three boxes define
24 the positions referred to in the text as Southern Indian Ocean (SIO), Southwestern
25 Pacific (SWP) and Southwestern Atlantic (SWA). Panel B. shows the opposite
26 relationship i.e. the area of negative 700 hPa temperature anomalies produced by
27 compositing months of positive 700 hPa geopotential height anomalies (thresholded
28 at the 90th percentile). The grid spacing is 15° in longitude and latitude. For reference,
29 the area of the Antarctic continent is 14 million km² and the area poleward of 65°S is
30 25 million km².

31

32 Applying the analysis used for Figures 4 and S2, we show in Figure S3 panel A (B)
33 the area of significant positive (negative) surface pressure anomalies south of 65°S
34 that is associated with positive (negative) surface pressure anomalies in each grid box.
35 The strongest association with Antarctic surface temperature anomalies is from
36 pressure anomalies of the same sign within the Antarctic region, which is distinctly
37 different to the association shown in Figure 4. Associations with the key centres
38 shown in Figure 4 are largely absent.

39

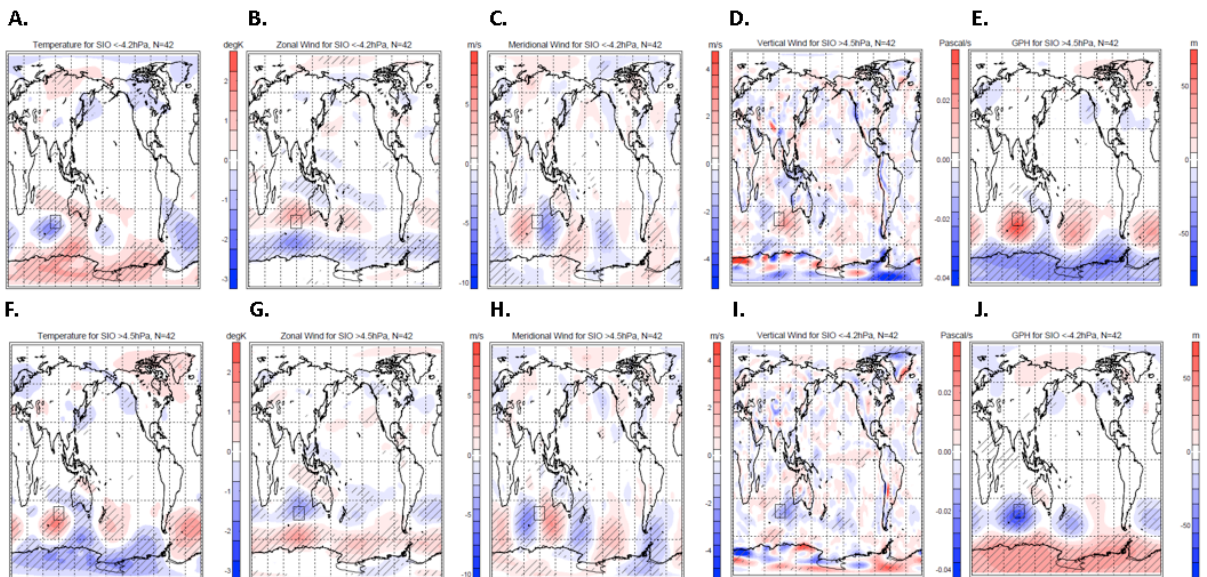


40

41 **Figure S3:** Panel A. The cumulative area of significant positive surface temperature
42 anomalies poleward of 65°S (in million km²) produced by compositing months of
43 positive surface pressure anomalies (thresholded at the 10th percentile) in each 10° x
44 10° (longitude x latitude) box, obtained from deseasonalised monthly ERA-Interim
45 reanalysis data for 1979-2012. Panel B. shows the opposite relationship i.e. the area of
46 negative temperature anomalies produced by compositing months of negative surface
47 pressure anomalies (thresholded at the 90th percentile). The grid spacing is 15° in
48 longitude and latitude.

49 *Text S3: Temperature Relationships with Zone Wave 3 Centres*

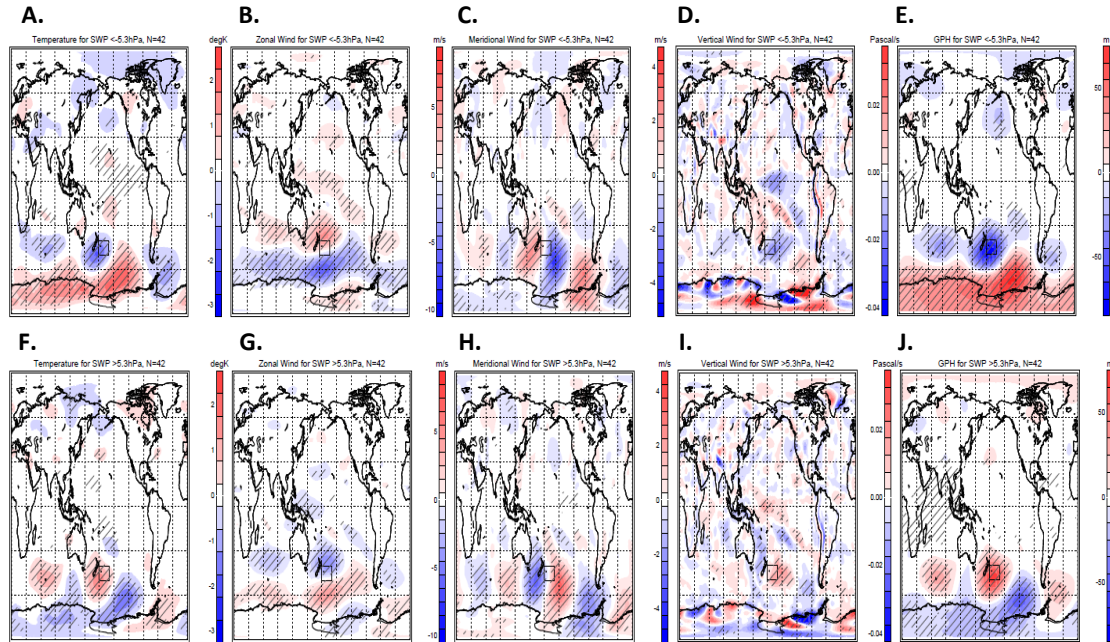
50 Composites were formed for deseasonalised sea level pressure (SLP) anomalies
51 averaged over the southern Indian Ocean (SIO) and southwestern Pacific (SWP)
52 regions identified in Figure 2 for deseasonalised values of surface temperature, zonal
53 and meridional wind speed, vertical pressure wind and geopotential height. Figures 6
54 and S4 relate to the SIO region using ERA-Interim and 20CR reanalysis, respectively,
55 while Figures 7 and S5 relate to the SWP region for ERA-Interim and 20CR
56 reanalyses, respectively. SLP anomalies were formed from each respective reanalysis
57 with respect to the 1979-2012 base period.



59 **Figure S4:** Composites of deseasonalised monthly 20CR reanalysis fields at 700 hPa
60 for surface pressure 10th percentile (negative) and 90th percentile (positive) anomalies
61 in the southern Indian Ocean (SIO) (80-100°E, 35-45°S) for 1979-2012. Shown are
62 temperature (A. and F.), zonal wind speed (B. and G.; positive = eastward) and
63 meridional wind speed (C. and H.; positive = northward), vertical pressure wind (D.
64 and I.; positive = downward) and geopotential height (E. and J.). The SIO surface
65 pressure anomaly threshold and the number of months (N) contributing to each

66 composite are shown at the top of each panel. Hatched areas denote areas of statistical
67 significance (95% confidence).

68



70 **Figure S5:** Composites of deseasonalised monthly 20CR reanalysis fields at 700 hPa
71 for surface pressure 10th percentile (negative) and 90th percentile (positive) anomalies
72 in the southwestern Pacific (SWP) Ocean (180-200°E, 45-55°S) for 1979-2012.
73 Shown are temperature (A. and F.), zonal wind speed (B. and G.; positive = eastward)
74 and meridional wind speed (C. and H.; positive = eastward), vertical pressure wind
75 (D. and I.; positive = downward) and geopotential height (E. and J.). The SWP
76 surface pressure anomaly threshold and the number of months (N) contributing to
77 each composite are shown at the top of each panel. Hatched areas denote areas of
78 statistical significance (95% confidence).

79

80

81

82 *Text S4: Overturning Circulation and Tropical Teleconnections*

83 We considered the influence of the surface pressure anomalies on the structure of the
84 overturning circulation by examining the meridional mass streamfunction. Figure 8
85 shows composites of the deseasonalised zonal mean streamfunction poleward of 15°S
86 for negative, positive and intermediate surface pressure anomalies in the SIO and
87 SWP regions. Generally, in comparison for the situation in the intermediate state, the
88 negative anomaly state shows a weakening (reduced volume) of the Polar cell and a
89 strengthening (increased volume) of the Ferrel cell (particularly on the poleward side
90 of the cell), which is consistent with increased poleward heat transport. For the
91 positive anomaly in comparison with the intermediate state, the Polar cell appears
92 slightly strengthened in the case of anomaly in the SIO region, while the Ferrel cell
93 appears slightly weaker in the case of the anomaly in the SWP region. While less
94 clear, the circulation changes in the positive state are consistent with reduced
95 poleward heat transport.

96

97 **References**

98

99

- 100 Dee, D. P., Uppala, S. M., Simmons, A. J., Berrisford, P., Poli, P., Kobayashi, S.,
101 Andrae, U., Balmaseda, M. A., Balsamo, G., Bauer, P., Bechtold, P., Beljaars, A. C.
102 M., van de Berg, L., Bidlot, J., Bormann, N., Delsol, C., Dragani, R., Fuentes, M.,
103 Geer, A. J., Haimberger, L., Healy, S. B., Hersbach, H., Hólm, E. V., Isaksen, L.,
104 Källberg, P., Köhler, M., Matricardi, M., McNally, A. P., Monge-Sanz, B. M.,
105 Morcrette, J. J., Park, B. K., Peubey, C., de Rosnay, P., Tavolato, C., Thépaut, J. N.,
106 and Vitart, F.: The ERA-Interim reanalysis: configuration and performance of the data
107 assimilation system, *Quarterly Journal of the Royal Meteorological Society*, 137, 553-
108 597, 2011.
109 Jouzel, J., Merlivat, L., Petit, J. R., and Lorius, C.: Climatic information over the last
110 century deduced from a detailed isotopic record in the South Pole snow, *Journal of
111 Geophysical Research*, 88, 2693-2703, 1983.
112